ChemComm

COMMUNICATION

View Article Online
View Journal | View Issue

Cite this: *Chem. Commun.*, 2014, **50**, 13604

Received 24th July 2014,
Accepted 16th September 2014

DOI: 10.1039/c4cc05768f

www.rsc.org/chemcomm

Simultaneous sensing of intracellular microRNAs with a multi-functionalized carbon nitride nanosheet probe†

Xianjiu Liao, Quanbo Wang and Huangxian Ju*

A multi-functionalized CNNS probe was designed by loading different dye-ssDNAs and folate on CNNSs, which was used for *in situ* fluorescence imaging and sensing of intracellular multiple microRNAs.

MicroRNAs (miRNAs) are a group of endogenous non-coding RNAs and play a significant role in regulating fundamental cellular processes through the modulation of gene expression.[1] The aberrant expression and misregulation of miRNAs have been found in various cancers.[2] Therefore, miRNAs have been regarded as biomarker candidates in clinical diagnosis and therapy.[3] Many techniques such as real-time quantitative PCR, northern blotting and microarrays have been used for miRNA analysis.[4] However, *in situ* monitoring of different miRNAs in living cells is still a challenge owing to the unique characteristics of miRNAs and collaborative regulation of multiple miRNAs in important cellular events.

Benefiting from the development of new materials, our previous studies proposed several systems for cellular delivery of recognition probes to monitor intracellular miRNA *via* confocal imaging.[5] Recently, graphene, a two-dimensional (2D) nanomaterial, has been extensively used in biological fields.[6] Bulk graphitic-phase carbon nitride (g-C_3N_4), as a representative 2D layered nanomaterial analogous to graphene, has also attracted great attention in the biosensing field.[7] Carbon nitride nanosheets (CNNSs) can be exfoliated from bulk g-C_3N_4 to directly disperse in aqueous solution without the need for surfactants or oxidation treatment, thus they hold great potential in biomedical applications.[8]

This work used CNNSs as a novel nanocarrier to design a multi-functionalized probe (mf-CNNS) for *in situ* monitoring of intracellular multiple miRNAs. As shown in Scheme 1A, the mf-CNNS was prepared by assembling different dye-labeled single-strand DNAs (dye-ssDNAs) and then folate (FA)-Poly A (ESI†) on CNNSs through their strong π–π interaction.[9] The loading of dye-ssDNAs on CNNSs led to the quenching of dye fluorescence (FL) by CNNSs,[9a] and the presence of FA on CNNSs achieved cell-target-specific delivery.[10] After the mf-CNNS was transfected into the cells, the hybridization of the assembled dye-ssDNAs with complementary targets weakened the π–π interaction between bases and CNNSs, which led to the release of the dye-ssDNAs from CNNSs, and thus recovered the quenched FL (Scheme 1B). The recovered FL could specifically respond to the complementary targets, leading to a sensing strategy for simultaneous detection of multiple miRNAs in a living cell.

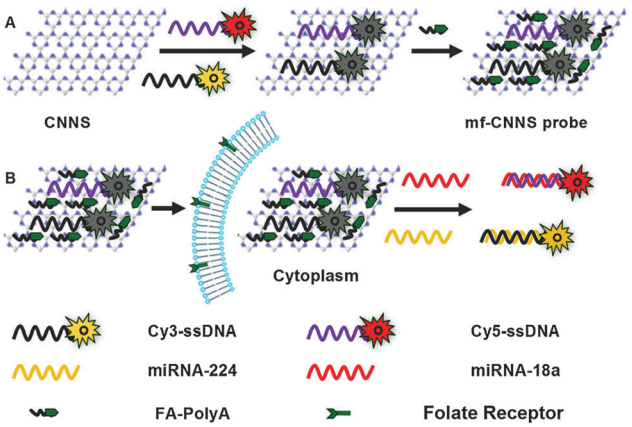

Scheme 1 Schematic illustration of (A) mf-CNNS probe preparation and (B) simultaneous detection of intracellular miRNAs with a mf-CNNS probe.

The FL spectrum of CNNS dispersion showed an emission peak at 463 nm at an excitation wavelength of 308 nm (Fig. S1, ESI†), thus the cell transfection could be monitored by the FL of CNNSs. The FL spectra did not change after dye-ssDNAs and folate was loaded on CNNSs, and the blue shift was also negligible with the increasing excitation wavelength (Fig. S2, ESI†). The FL intensity of CNNSs was slightly affect by time, ionic strength and temperature and showed pH-dependent behaviour (Fig. S3 and S4, ESI†). The X-ray diffraction pattern of CNNSs showed the g-C_3N_4 crystal peak at 27.7 degree,[8] and

State Key Laboratory of Analytical Chemistry for Life Science, School of Chemistry and Chemical Engineering, Nanjing University, Nanjing 210093, P.R. China. E-mail: hxju@nju.edu.cn; Fax: +86 25 83593593; Tel: +86 25 83593593

† Electronic supplementary information (ESI) available: Experimental details and additional figures. See DOI: 10.1039/c4cc05768f

the X-ray photoelectron spectrum showed a nitrogen to carbon ratio of 1.36 (Fig. S5, ESI†), close to the theoretical value of 1.33,[9a] indicating its high purity. The TEM of CNNSs clearly showed a planar structure with a nearly transparent feature (Fig. S6A, ESI†), indicating its ultrathin thickness with a dimension of around 140 nm (Fig. S7A, ESI†).[8] The relatively negative zeta potential of −28.5 mV (Fig. S6B, ESI†) led to a good dispersity in water, which was favourable for biosensing application. After dye-ssDNAs were assembled on CNNSs, the absorption spectrum showed Cy3 and Cy5 characteristic peaks and remarkable hypochromicity[9a] (Fig. S7B, ESI†), and the zeta potential became more negative due to the negatively-charged phosphate of ssDNA.[9a] The loading of FA-Poly A on m-CNNSs led to more negative zeta potential (Fig. S6B, ESI†), which confirmed the successful preparation of the mf-CNNS probe.

The FL quenching ability of CNNSs on the dyes and the release of dye-ssDNAs from the CNNS surface upon hybridization with complementary miRNA were firstly examined. After Cy3-ssDNA or Cy5-ssDNA was mixed with an increasing amount of CNNSs, the FL of dyes gradually decreased (Fig. S8, ESI†), indicating the quenching effect of CNNSs on the FL of both Cy3 and Cy5. The quenching could be attributed to the static electronic communication between dyes and CNNSs.[9a,11] The addition of complementary miRNA into the corresponding mixture led to the recovery of dye FL. Although the excessive miRNA was added in the mixture, the FL recovery efficiency decreased with the increasing amount of CNNSs. Considering the quenching and recovery efficiency of dye FL, a 100 μg mL^{-1} CNNS at 50 nM Cy3-ssDNA or Cy5-ssDNA was selected as the optimal condition for the detection of miRNAs.

Synchronous scanning spectra of Cy3-ssDNA and Cy5-ssDNA were further recorded to examine the FL change. CNNS dispersion did not show an obvious FL peak in the examined range from 500 to 750 nm, however, it showed a strong quenching effect on the FL of both Cy3-ssDNA and Cy5-ssDNA (Fig. 1A). Moreover, the quenching efficiency increased with the increasing amount of CNNSs. Upon addition of miRNA-18a and miRNA-224 to the suspension of the mf-CNNS probe, the FL intensity of Cy3 and Cy5 increased without interfering each other (Fig. 1B), indicating the specific recognition of dye-ssDNAs on the mf-CNNS probe to complementary miRNAs, which formed a DNA–miRNA duplex helix to weaken the π–π interaction between the bases and CNNSs, and thus led to the efficient release of the dye-ssDNAs from the probe to emit FL. The differentiable FL recovery of two dyes provided a simple method for simultaneous detection of these miRNAs.

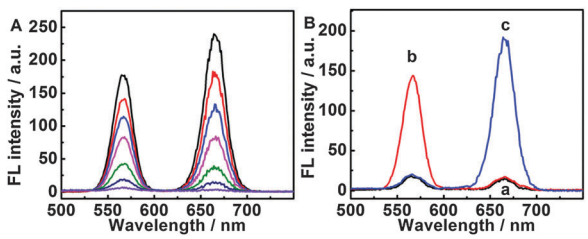

Fig. 1 Synchronous scanning FL spectra of (A) 50 nM Cy3-ssDNA and Cy5-ssDNA after incubation with 0, 40, 80, 120, 160 and 200 μg mL^{-1} CNNSs at 37 °C for 5 min and 200 μg mL^{-1} CNNS (from top to bottom), and (B) a 200 μg mL^{-1} mf-CNNS probe (a) after incubation with 250 nM miRNA-224 (b) and miRNA-18a (c) at 37 °C for 1 h. The synchronous scanning spectra are excited at 478 nm. All measurements are performed in HB.

The formation of a dye-DNA–miRNA duplex helix could be confirmed with polyacrylamide gel electrophoresis analysis (Fig. S9, ESI†). This system displayed sequence specificity for discriminating the complementary target from the three- and single-base mismatched and non-complementary sequence (Fig. S10, ESI†). The complementary target showed the FL recovery of about 3.0 and 4.0 times that of the single- and three-base mismatch sequence, respectively, and the FL change of mf-CNNSs upon addition of the non-complementary sequence was negligible.

Oligonucleotides are susceptible to degradation by cellular nucleases during delivery into the cells. Therefore, an efficient delivery vector should protect the cargo against nuclease digestion and SSB interaction during prolonged transport. Herein, the ability of CNNSs to protect the ssDNA from nuclease cleavage and interfering proteins was studied. The mf-CNNS suspension presented low fluorescence intensity. After incubation with miRNA-224 or miRNA-18a, a sharp increase of FL from the Cy3 or Cy5 was observed (Fig. S11, ESI†), while both 250 nM SSB and 1.0 unit DNase I showed the FL increase of 9.8/9.4% and 11.8/11.3% resulting from the complementary miRNA-224/miRNA-18a, respectively. Thus CNNSs could well resist DNase I cleavage and SSB interaction. The protection could be attributed to the shielding from the CNNS or the conformational change of nucleic acid strands when adsorbed on the CNNS surface.[12]

To exactly evaluate the cytotoxicity of a gene carrier with MTT assay, HepG2 cells were treated with folate functionalized CNNSs (f-CNNSs) from 50 to 800 μg mL^{-1} for 3 h, which exhibited the viability from 98.7% to 90.9% (Fig. S12A, ESI†), suggesting that CNNSs possessed low cytotoxicity. The viability of cells transfected with f-CNNSs was even higher than those transfected with an f-carbon nanosphere (f-CNS) and f-graphene oxide (f-GO) (Fig. S12B, ESI†), indicating lower cytotoxicity of the CNNS than CNS and GO.

The cell-specific transfection of f-CNNSs in living cells could be monitored by the photoluminescence of CNNSs. As shown in Fig. S13 (ESI†), with the increasing incubation time of HepG2 cells with f-CNNS suspension, the transfected cells showed increasing FL of CNNSs (column A), indicating the increasing uptake of f-CNNSs. However, the HepG2 cells transfected with CNNSs showed negligible FL (column B). Thus the presence of FA on CNNSs was necessary for cell-specific transfection due to the presence of a folate receptor (FR) overexpressed on cancer cells. The FR-mediated endocytosis of f-CNNSs could be further confirmed with A549 cells (FR-negative cells, column C) and HaCaT cells (non-cancerous cells, column D), which also showed very low FL of CNNSs (Fig. S14, ESI†).

Colocalization experiments were performed to demonstrate the endosomal escape of mf-CNNSs. After HepG2 cells were incubated with mf-CNNSs and Hoechst 333342, the cells showed strong Cy5 FL in the cytoplasm due to the hybridization of Cy5-ssDNA on the probe with miRNA-18a (Fig. 2a), indicating the presence of miRNA and mf-CNNSs in the cytoplasm. The mf-CNNS and LysoTracker

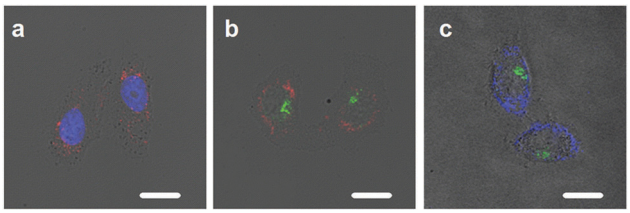

Fig. 2 Confocal microscopic images of HepG2 cells transfected with 200 μg mL^{-1} mf-CNNS for 3 h and then 1.0 μM Hoechst 333342 for 20 min (a), 200 μg mL^{-1} mf-CNNS (b) and f-CNNS (c) probe for 3 h and then 1.0 μM LysoTracker Green DND-26 for 20 min at 37 °C. Scale bars: 20 μm.

Green DND-26 transfected HepG2 cells showed strong Cy5 FL without colocalization with endocytic vesicles in the cytoplasm (Fig. 2b), indicating that the mf-CNNS probe successfully escaped from endocytic vesicles to recognize miRNA-18a in the cytoplasm.[13] The f-CNNS and LysoTracker Green DND-26 transfected HepG2 cells also showed strong CNNS FL without colocalization with endocytic vesicles in the cytoplasm (Fig. 2c), indicating the successful endosomal escape and efficient cytoplasmic diffusion of f-CNNSs.

To investigate the capability of mf-CNNSs for simultaneously monitoring intracellular multiple miRNAs, the incubation time and the amount of mf-CNNSs were optimized to be 3 h and 200 μg mL^{-1} with confocal microscopy (Fig. S15, ESI†). After HepG2 cells were incubated with different miRNA inhibitors to induce different levels of miRNAs, they were incubated with mf-CNNSs for 3 h and subsequently analyzed by confocal microscopy. The cells exhibited strong FL signals of both Cy3 and Cy5 (Fig. 3A), indicating high levels of both miRNA-224 and miRNA-18a in HepG2 cells.[14] After HepG2 cells were incubated with inhibitor-224 and inhibitor-18a (Fig. 3B), the miRNA-224 and miRNA-18a levels showed 50.0% and 46.6% down-regulation (Fig. S16, ESI†), respectively. When HepG2 cells were incubated with only inhibitor-224 (Fig. 3C) or inhibitor-18a (Fig. 3D), the miRNA-224 or the miRNA-18a level showed 51.3% or 48.1% down-regulation (Fig. S16, ESI†), respectively, while the expression level of miRNA-18a or miRNA-224 did not change. In parallel monitoring, HeLa cells showed 72.6% and 77.6% of the miRNA-224 and miRNA-18a expression levels of HepG2 cells (Fig. 3D), respectively. Thus, the proposed method could be used for *in situ* monitoring of the dynamic changes in intracellular multiple miRNAs.

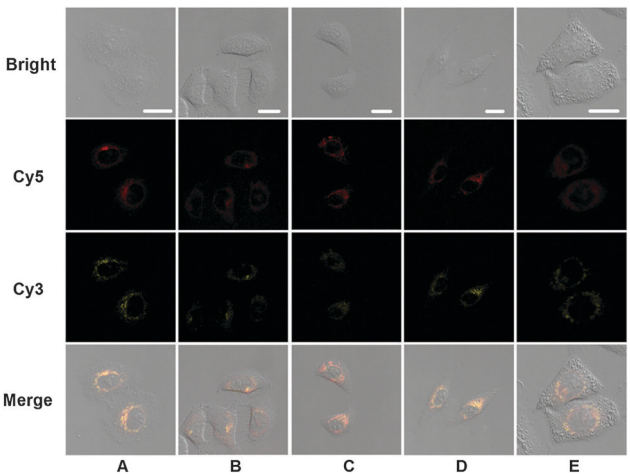

Fig. 3 Simultaneous monitoring of miRNA-224 (Cy3) and miRNA-18a (Cy5) with confocal microscopic images of HepG2 cells (A), HepG2 cells treated with 50 nM inhibitors-18a and inhibitor-224 (B), 50 nM inhibitor-224 (C), 50 nM inhibitor-18a (D) for 48 h and HeLa cells (E) and then transfected with a 200 μg mL^{-1} mf-CNNS probe at 37 °C for 3 h. Scale bars: 20 μm.

To confirm the detection results with the proposed method, flow cytometric analysis was performed for intracellular miRNA detection. The miRNA-224 and miRNA-18a levels of HepG2 cells incubated with both inhibitor-224 and inhibitor-18a showed 47.7% and 48.8% down-regulation, respectively (Fig. S17 and S18, ESI†). Single inhibitor-224 or inhibitor-18a led to 49.2% or 50.2% down-regulation of miRNA-224 or miRNA-18a, while miRNA-18a or miRNA-224 remained at the original expression level (Fig. S17 and S18, ESI†). HeLa cells showed 69.1% and 78.7% of the miRNA-224 and miRNA-18a expression levels in HepG2 cells (Fig. S17 and S18, ESI†), respectively. These results were in good agreement with those obtained with the proposed method, indicating good validation.

This work successfully assembled two dye-ssDNAs and FA on CNNSs to design an mf-CNNS for target-cell-specific monitoring of multiple intracellular miRNAs. The CNNS showed low cytotoxicity and a strong FL quenching ability on the dye labels, which could be recovered upon the specific recognition of the dye-ssDNA to miRNA due to the release of the formed DNA–miRNA duplex helix from the CNNS surface. The good protection properties of CNNSs for avoiding nuclease digestion and SSB interaction of ssDNA led to a specific method for *in situ* monitoring of multiple intracellular miRNAs. The designed sensing strategy realized the simultaneous detection of multiple miRNAs in living cells. In virtue of these advantages, the proposed strategy implied the potential for biomedical research and clinical diagnostics.

This research was financially supported by the National Basic Research Program of China (2010CB732400), and the National Natural Science Foundation of China (21135002, 21121091).

Notes and references

1 (*a*) R. H. Plasterk, *Cell*, 2006, **124**, 877–881; (*b*) D. P. Bartel, *Cell*, 2004, **116**, 281–297; (*c*) H. F. Dong, J. P. Lei, L. Ding, Y. Q. Wen, H. X. Ju and X. J. Zhang, *Chem. Rev.*, 2013, **113**, 6207–6233.
2 (*a*) A. Ventura and T. Jacks, *Cell*, 2009, **136**, 586–591; (*b*) N. Kosaka, H. Iguchi and T. Ochiya, *Cancer Sci.*, 2010, **101**, 2087–2092; (*c*) J. J. Rossi, *Cell*, 2009, **137**, 990–992; (*d*) A. Esquela-Kerscher and F. J. Slack, *Nat. Rev. Cancer*, 2006, **6**, 259–269.
3 (*a*) A. Gupta, J. J. Gartner, P. Sethupathy, A. G. Hatzigeorgiou and N. W. Fraser, *Nature*, 2006, **442**, 82–85; (*b*) C. C. Pritchard, H. H. Cheng and M. Tewari, *Nat. Rev. Genet.*, 2012, **13**, 358–369.
4 (*a*) J. Li, B. Yao, H. Huang, Z. Wang, C. H. Sun, Y. Fan, Q. Chang, S. L. Li, X. Wang and J. Z. Xi, *Anal. Chem.*, 2009, **81**, 5446–5451; (*b*) G. S. Pall, C. Codony-Servat, C. J. Byrne, L. Ritchie and A. Hamilton, *Nucleic Acids Res.*, 2007, **35**, e60; (*c*) P. T. Nelson, D. A. Baldwin, L. M. Scearce, J. C. Oberholtzer, J. W. Tobias and Z. Mourelatos, *Nat. Methods*, 2004, **1**, 155–161; (*d*) J. M. Lee and Y. W. Jung, *Angew. Chem., Int. Ed.*, 2011, **50**, 12487–12490.
5 (*a*) H. F. Dong, L. Ding, F. Yan, H. X. Ji and H. X. Ju, *Biomaterials*, 2011, **32**, 3875S–3882S; (*b*) H. F. Dong, J. P. Lei, H. X. Ju, F. Zhi, H. Wang, W. J. Guo, Z. Zhu and F. Yan, *Angew. Chem., Int. Ed.*, 2012, **51**, 4607–4612.

6 (*a*) S. J. He, B. Song, D. Li, C. F. Zhu, W. P. Qi, Y. Q. Wen, L. H. Wang, S. P. Song, H. P. Fang and C. H. Fan, *Adv. Funct. Mater.*, 2010, **20**, 453–459; (*b*) S. S. Chou, M. De, J. Luo, V. M. Rotello, J. Huang and V. P. Dravid, *J. Am. Chem. Soc.*, 2012, **134**, 16725–16733; (*c*) Y. Wang, Z. H. Li, D. H. Hu, C. T. Lin, J. H. Li and Y. H. Lin, *J. Am. Chem. Soc.*, 2010, **132**, 9274–9276.

7 (*a*) C. M. Cheng, Y. Huang, X. Q. Tian, B. Z. Zheng, Y. Li, H. Y. Yuan, D. Xiao, S. P. Xie and M. M. F. Choi, *Anal. Chem.*, 2012, **84**, 4754–4759; (*b*) C. M. Cheng, Y. Huang, J. Wang, B. Z. Zheng, H. Y. Yuan and D. Xiao, *Anal. Chem.*, 2013, **85**, 2601–2605.

8 X. D. Zhang, X. Xie, H. Wang, J. J. Zhang, B. C. Pan and Y. Xie, *J. Am. Chem. Soc.*, 2013, **135**, 18–21.

9 (*a*) Q. B. Wang, W. Wang, J. P. Lei, N. Xu, F. L. Gao and H. X. Ju, *Anal. Chem.*, 2013, **85**, 12182–12188; (*b*) C. H. Lu, H. H. Yang, C. L. Zhu, X. Chen and G. N. Chen, *Angew. Chem., Int. Ed.*, 2009, **121**, 4879–4881.

10 (*a*) K. Kogure, R. Moriguchi, K. Sasaki, M. Ueno, S. Futaki and H. J. Harashima, *J. Controlled Release*, 2004, **98**, 317–323; (*b*) C. P. Leamon, M. A. Parker, I. R. Vlahov, L. C. Xu, J. A. Reddy, M. Vetzel and N. Douglas, *Bioconjugate Chem.*, 2002, **13**, 1200–1210.

11 S. A. E. Marras, F. R. Kramer and S. Tyagi, *Nucleic Acids Res.*, 2002, **30**, e122.

12 Y. R. Wu, J. A. Phillips, H. P. Liu, R. H. Yang and W. H. Tan, *ACS Nano*, 2008, **2**, 2023–2028.

13 (*a*) A. K. Varkouhi, M. Scholte, G. Storm and H. J. Haisma, *J. Controlled Release*, 2011, **150**, 220–228; (*b*) M. Huang, C. W. Fong, E. Khor and L. Y. Lim, *J. Controlled Release*, 2005, **106**, 391–406.

14 (*a*) Y. Wang, A. T. Lee, J. Z. Ma, J. Wang, J. Ren, Y. Yang, E. Tantoso, K. B. Li, L. L. Ooi, P. Tan and C. G. Lee, *J. Biol. Chem.*, 2008, **283**, 13205–13215; (*b*) Y. Murakami, T. Yasuda, K. Saigo, T. Urashima, H. Toyoda, T. Okanoue and K. Shimotohno, *Oncogene*, 2006, **25**, 2537–2545.